

**RAK-2****NKS/RAK-2(97)TR-A5****ISBN 87-7893-033-2**

**PARAMETRIC STUDIES ON CONTAINMENT THERMAL  
HYDRAULIC LOADS DURING HIGH PRESSURE MELT  
EJECTION IN A BWR**

**A. Silde  
I. Lindholm**

**VTT Energy  
Espoo, Finland**

**December 1997**

**Informationsservice, Risø, 1998**

**NKS/RAK-2(97)TR-A5  
ISBN 87-7893-033-2**

**Rapporten er udgivet af:  
NKS-sekretariatet  
Bygning 100  
Postboks 49  
DK-4000 Roskilde**

**Tlf. +45 4677 4045  
Fax +45 4677 4046  
E-mail [annette.lemmens@risoe.dk](mailto:annette.lemmens@risoe.dk)  
<http://www.risoe.dk/nks>**

# ABSTRACT

The containment thermal hydraulic loads during high pressure melt ejection in a Nordic BWR are studied parametrically with the CONTAIN and the MELCOR codes. The work is part of the Nordic RAK-2 project.

The containment analyses were divided into two categories according to composition of the discharged debris: metallic and oxidic debris cases. In the base case with highly metallic debris, all sources from the reactor coolant system to the containment were based on the MELCOR/BH calculation. In the base case with the oxidic debris, the source data was specified assuming that ~ 15 % of the whole core material inventory and 34 000 kg of saturated water was discharged from the reactor pressure vessel (RPV) during 30 seconds. In this case, the debris consisted mostly of oxides.

The highest predicted containment pressure peaks were about 8.5 bar. In the scenarios with highly metallic debris source, very high gas temperature of about 1900 K was predicted in the pedestal, and about 1400 K in the upper drywell. The calculations with metallic debris were sensitive to model parameters, like the particle size and the parameters, which control the chemical reaction kinetics.

In the scenarios with oxidic debris source, the predicted pressure peaks were comparable to the cases with the metallic debris source. The maximum gas temperatures (about 450-500 K) in the containment were, however, significantly lower than in the respective metallic debris case. The temperatures were also insensitive to parametric variations.

In addition, one analysis was performed with the MELCOR code for benchmarking of the MELCOR capabilities against the more detailed CONTAIN code.

The calculations showed that leaktightness of the containment penetrations could be jeopardized due to high temperature loads, if a high pressure melt ejection occurred during a severe accident. Another consequence would be an early containment venting.

# TABLE OF CONTENTS

ACKNOWLEDGEMENTS .....	1
EXECUTIVE SUMMARY .....	2
1. INTRODUCTION .....	5
2. OBJECTIVES .....	6
3. BACKGROUND .....	7
3.1 Phenomena of High Pressure Melt Ejection .....	7
3.2 High Pressure Melt Ejection in Nordic BWRs .....	8
4. TECHNICAL APPROACH .....	11
5. CONTAIN AND MELCOR CODES .....	12
5.1 DCH Models .....	12
5.2 Main Limitations of the DCH Models .....	16
6. OLKILUOTO PLANT MODEL .....	17
6.1 Initial Accident Sequence .....	17
6.2 Reactor Coolant System .....	17
6.3 Containment .....	18
7. PRESSURE VESSEL LOWER PLENUM CONDITIONS AT VESSEL BREACH .....	21
8. CONTAINMENT RESPONSE .....	24
8.1 Metallic Debris Source .....	24
8.1.1 Code Benchmark Case .....	24
8.1.2 Sensitivity Calculations .....	27
8.2 Oxidic Debris Source .....	31
9. CONCLUSIONS .....	35
10. REFERENCES .....	36
DISTRIBUTION LIST .....	39

## **ACKNOWLEDGEMENTS**

This work was partially sponsored by the Finnish Ministry of Trade and Industry (KTM) which is gratefully acknowledged.

The authors are indebted to Mr. Heikki Sjövall (TVO) for technical support and constructive comments on the work. Special thanks are also to Mr. Risto Sairanen (VTT) for reviewing the document.

# EXECUTIVE SUMMARY

The main focus of the Nordic RAK-2 project has been on the assessment of in-vessel melt progression phenomena in Nordic BWRs. In some severe accident sequences, the lower head breach of RPV may occur at high reactor coolant system pressure leading to high pressure melt ejection (HPME). When the ejected debris material is dispersed into the containment gas volume, a large amount of energy is released from hot particles to the containment atmosphere. In addition, the exothermic chemical reactions of the metallic debris components with steam and oxygen will increase the containment loading. These heating processes are known as direct containment heating (DCH). Generally, the severity of the containment loads during HPME are strongly coupled with the progression of in-vessel core degradation processes, failure pressure of reactor pressure vessel, and lower head failure modes. The debris transport and dispersal processes are also very dependent on the containment geometry.

HPME phenomena in BWRs have not received the same attention as in PWRs, mainly because the probability of pressure vessel failure at high reactor coolant system pressure is low due to reliable Automatic Depressurization System (ADS) in BWRs. However, if the containment fails from the HPME loads, radiological consequences could be serious.

The debris dispersal method in BWRs is different from the DCH scenarios envisaged for PWRs. In a BWR, the vessel will fail most likely from the instrument tube penetrations with a small initial hole. Our assumption is that the discharging melt may be dispersed directly to the containment atmosphere, when entering relatively large pedestal atmosphere during the first few tens of seconds of the blowdown. This assumption was the basis of our study. In a PWR case, a large amount of melt is generally assumed to be discharged from the reactor pressure vessel at a pressure that can be twice as high as the normal operation pressure of a BWR. The debris is ejected to the cavity floor beneath the vessel lower head and the steam/water blowdown following after may entrain and disperse a certain fraction of the melt into the containment atmosphere.

The objective of this study is to evaluate the containment pressure and temperature loads involved with the high pressure melt ejection in Olkiluoto BWR units. These studies also extend the earlier DCH work performed in level 2 PSA at TVO.

This study concentrates only on the thermal-hydraulic loads during the high pressure melt ejection. Because the Nordic BWR containments are inerted with nitrogen, hydrogen combustion phenomena were not addressed. The critical points in pedestal leaktightness are the various penetrations in the lower drywell. If the pedestal is flooded prior to HPME, the penetrations are secured by surrounding water, and only the leaktightness of the upper drywell penetrations may be jeopardized by hot gases. In case of a dry pedestal, the pedestal penetrations are exposed to thermal attack by the hot gases or the debris particles. Fuel coolant interaction in the pedestal water pool was out of scope of the study.

The containment analyses were divided into two categories according to composition of the discharged debris: metallic and oxidic debris cases. In the base case with highly metallic debris, all sources from the reactor coolant system to the containment were based on the MELCOR/BH calculation. In the base case with the oxidic debris, the source data was specified assuming that ~ 15 % of the whole core material inventory and 34 000 kg of saturated water was discharged from the RPV during 30 seconds. In this case, the debris consisted mostly of oxides.

The highest predicted containment pressure peaks were about 8.5 bar. In the scenarios with highly metallic debris source, very high gas temperatures of about 1900 K were predicted in the pedestal, and about 1400 K in the upper drywell. The high temperatures were consequences of the highly superheated steam released simultaneously with debris from reactor pressure vessel, and of the heat released from the oxidation of metallic debris particles. However, the calculations with metallic debris were sensitive to model parameters, like the particle size and parameters, which control the chemical reaction kinetics.

In the scenarios with oxidic debris source, the predicted pressure peaks were comparable to the cases with the metallic debris source. The maximum gas temperatures (about 450-500 K) in the containment were however significantly lower than in the respective metallic debris case. The temperatures were also insensitive to parametric variations. This can be explained by the cooling effect of steam, which is produced in the oxidic debris scenario by flashing of the saturated blowdown water. The containment gas temperature was determined by the large amount of saturated steam, not the Direct Containment Heating processes. Due to minor effect of DCH on the containment temperature loads, the influence of model parameter variations was also insignificant.

Although CONTAIN was the main tool in the containment analyses, one containment calculation was performed with the MELCOR code for benchmarking of the MELCOR capabilities against more detailed CONTAIN code. In the comparison case, MELCOR predicted ~ 1.5 bar higher pressure maximum than CONTAIN (8 versus 6.5 bar). The predicted gas temperatures also behaved differently. One reason for that was the limitation of MELCOR in modelling the intercell transport of the airborne debris. The user must therefore specify a set of debris destinations and corresponding fractions that prescribe, where the ejected debris is assumed to go. In the CONTAIN calculation, most of the debris particles (~ 95%) were trapped and deposited in the pedestal. The rest of the particles were cooled in the pedestal atmosphere prior flowing to the upper drywell. Despite the conservative assumption used in the CONTAIN calculation (infinite drop-side diffusivity), MELCOR predicted more complete and intensive chemical reactions than CONTAIN. MELCOR estimated ~ 350 kg hydrogen production during the debris discharge. Corresponding CONTAIN estimate was ~ 165 kg.

The CONTAIN DCH model is much more mechanistic than the MELCOR FDI/HPME DCH model, which has a fully parametric approach. For example, MELCOR does not handle the intercell debris transport and the debris particle can be removed only by gravitational settling. CONTAIN is therefore recommended as a best-estimate code for DCH containment analyses. If the loading induced by DCH is primarily limited by the amount of thermal and chemical energy available in the debris, also the MELCOR model can be adequate for parametric PSA studies.

The calculations showed that if a high pressure melt ejection occurred during a severe accident, it could jeopardize leaktightness of the containment penetrations due to high temperature loads. Another consequence would be an early containment venting.

# 1. INTRODUCTION

The main focus of the Nordic RAK-2 project has been on the assessment of in-vessel melt progression phenomena in Nordic BWRs. These studies have covered the coolability of a degraded core by reflooding in the core region, the possible consequences of reflooding, e.g. recriticality, and finally the assessment of late phase melt progression, where the core melt migrates into the lower head potentially leading to reactor pressure vessel failure and core debris discharge into the containment. In some severe accident sequences, the lower head breach of the RPV may occur at high reactor coolant system pressure leading to high pressure melt ejection (HPME). When the debris material is dispersed into the containment atmosphere, a large amount of energy is released from hot particles to the containment atmosphere. In addition, the exothermic chemical reactions of the metallic debris components with steam and oxygen will increase the containment loading. These heating processes are known as direct containment heating (DCH). Generally, the severity of the containment loads during HPME are strongly coupled with the progression of in-vessel core degradation processes, reactor coolant system pressure, and the lower head failure mode. Debris transport and dispersal processes are also dependent on the containment geometry.

The mechanisms for containment loading during HPME may include the addition of vapor and non-condensable gases to the containment atmosphere (blowdown), the rapid release of thermal and chemical energy to atmosphere, hydrogen combustion, and rapid vaporization of pool water due to fuel coolant interaction in the cavity. In addition, the containment barrier may be challenged by a missile generation and a direct thermal attack on the containment structures by molten debris.

HPME phenomena in BWRs have not received the same attention as in PWRs, mainly because the probability of the pressure vessel failure at high reactor coolant system pressure is low due to reliable Automatic Depressurization System (ADS) used in BWRs. However, if the containment fails from the HPME loads, radiological consequences could be serious. The consequences of DCH have therefore been studied in level 2 PSA for Olkiluoto 1 and 2 BWR units (Sjövall, 1997, Keinänen, 1996).

The debris dispersal method in BWRs is different from the DCH scenarios envisaged for PWRs. In a BWR, the vessel will fail most likely from the instrument tube penetrations with a small initial hole. Our basic assumption is that the discharging melt is dispersed directly into the containment atmosphere, when entering a relatively large pedestal atmosphere during the first few tens of seconds of the blowdown. In a PWR case, a large amount of melt is generally assumed to be discharged from the reactor pressure vessel at a pressure that can be twice as high as the normal operation pressure of a BWR. The debris is ejected to the cavity floor beneath the vessel lower head and the steam/water blowdown following after may entrain and disperse a certain fraction of the melt into the containment atmosphere.

This study concentrates only on the thermal-hydraulic loads during the high pressure melt ejection. Because the Nordic BWR containments are inerted with nitrogen, hydrogen combustion phenomena were not addressed. Neither the fuel coolant interaction in the pedestal water pool was handled in the study.

## 2. OBJECTIVES

The objective of this study was to evaluate the containment thermal hydraulic loads in Olkiluoto BWR units in case of a high pressure melt ejection and direct containment heating.

The probability to HPME is very small due to the depressurization system used in BWRs. A scoping study was considered useful because rapid pressurization may challenge the containment integrity or may lead to early containment venting. In addition, high temperature loads may jeopardize the leaktightness of the containment penetrations leading to a long term leak-path directly from the containment to the environment.

One aim of the study was also to extend the earlier DCH studies performed at TVO in level 2 PSA for Olkiluoto BWR units (Sjövall, 1997) by performing additional sensitivity analyses with the CONTAIN code. Lumped parameter codes, like MELCOR and CONTAIN, have inherent limitations, e.g. related to material transportation and trapping within complex geometries. The CONTAIN and MELCOR code developers have introduced several correlations to describe DCH phenomena with a set of user specified sensitivity parameters to circumvent the limitations. This study, therefore, focused on performing a number of CONTAIN calculations varying some key model parameters and physical boundary conditions.

Although CONTAIN was the main tool in the containment analyses, one containment calculation was performed with the MELCOR code for benchmarking of the code capabilities against the more detailed CONTAIN code. The application of the simple MELCOR model is justified by the fact that the code is currently the main tool for integral severe accident calculations for Olkiluoto NPP.

## 3. BACKGROUND

### 3.1 Phenomena of High Pressure Melt Ejection

In some core melt accidents, the reactor pressure vessel may fail while the reactor coolant system is still at high pressure leading to high pressure melt ejection (HPME). The core melt may be dispersed into the containment resulting in the pressurization and heating of the containment atmosphere. These heating processes are known as direct containment heating (DCH).

Generally, the severity of the containment loads during HPME are strongly coupled with the progression of in-vessel core degradation processes, the pressure at failure of RPV, and lower head failure modes. The debris transport and dispersal processes are also very dependent on the containment geometry. An excellent overview of the main phenomena in case of a HPME can be found e.g. in reference (Fontana, 1993).

Possible containment loading mechanisms during HPME are:

- 1) Blowdown phase: rapid addition of water, vapour and non-condensable gases to the containment atmosphere leading to static or dynamic pressure loads for the containment structures.
- 2) Energetic discharge of the debris melt from the RPV: transportation and dispersal of the debris particles leading to rapid thermal and chemical energy release into the containment atmosphere (DCH). The pressure loads in the cavity are probably dynamic during the debris discharge.
- 3) Combustion of pre-existing and released hydrogen in the containment.
- 4) Rapid vaporization of cavity water due to melt-water interaction.
- 5) Direct attack of the molten debris on the containment structures.
- 6) Missile generation.

The effect of direct containment heating is only of interest if a significant fraction of the debris can be transported and dispersed into the containment atmosphere. The main work has focused on the dispersal mechanisms of molten debris from the PWR reactor cavities of different geometries. The debris dispersal is viewed as one of the most important factors affecting the containment loading in PWRs during HPME. For example, the IDCOR project categorized existing PWR reactor cavities in order to assess how much of the debris could be dispersed from the cavity to the containment atmosphere (IDCOR, 1985).

The research of HPME and DCH was actually started in the Zion Probabilistic Safety Study. The probability of containment failure by DCH for the Zion plant was extensively assessed in references (Pilch, 1994a and Pilch et al., 1994b). Several integral and separate effect tests have been conducted to resolve this issue e.g. at Sandia (SNL) and Argonne (ANL) National Laboratories, and Fauske and Associates (FAI) (NEA, 1996, Blanchat & Allen, 1995). Also some scaled experiments are performed in the United Kingdom using simulant materials. The integral effect IET-tests were conducted by SNL at the Surtsey Facility using 1:10 linear scale models of Zion (designated as IET-1 - IET-8 experiments), and under more prototypic conditions with the 1:6 scale model

of Surry (IET-9 - IET-11) (Blanchat & Allen, 1995). These tests were funded by USNRC. A high-temperature, chemically reactive melt is discharged by high-pressure steam into the model cavity. Effects of many specific phenomena e.g. water in the cavity, hydrogen combustion, and the sub-compartment structures on the containment pressurization have been studied (Allen et al., 1992a,b,c, Allen et al, 1993a,b). The tests showed that the combustion of hydrogen produced by steam/metal reactions contributed significantly to containment pressurization if the atmosphere was not inerted. Hot jet of hydrogen was observed to burn as a diffusion flame as it was pushed into air atmosphere in the upper dome of facility. Water on the basement floor did not appear to have a significant effect on the peak pressure. The IET tests also demonstrated the importance of the sub-compartment structures to trap the debris particles prior to dispersal to the upper dome atmosphere.

All the experiments were focused on PWR conditions. Since the issue is highly plant dependent, extrapolation of the test results to BWRs is difficult. A good example of the sensitivity of the results to initial conditions are the IET-experiments. The measured pressure increase varied from 87 to 430 kPa depending on the initial conditions and the geometry used (Blanchat & Allen, 1995). Only the experiments IET-1 and IET-1R were performed in fully inerted atmosphere ( $< 0.2$  mol. %  $O_2$ ), which approximately corresponds to typical conditions in Nordic BWR containments. The nitrogen inerting prevented the hydrogen combustion and contribution to the vessel pressurization. The measured pressure peaks in IET-1 and IET-1R were  $\sim 100$  kPa. This is significantly lower than in IET-3 (246 kPa), where the facility was not inerted ( $\sim 9$  mol. %  $O_2$ ).

The HIPS tests indicated that a large quantity of water may not be an efficient heat sink for DCH (Tarbell, 1991). This conclusion is, however, set questionable since in the HIPS tests most of the water escaped as a plug from the cavity prior to melt dispersal (Blanchat & Allen, 1995).

Rapid debris discharge into water may lead to energetic metal-water interaction and following steam generation. The pressure peaks in some of the IET experiments were supposed to be caused by a steam explosion following the melt-water interaction in the cavity. The issues involved with the water effect during HPME can still be viewed as unsolved.

### **3.2 High Pressure Melt Ejection in Nordic BWRs**

HPME phenomena in BWRs have not received the same attention as in PWRs, mainly because the probability of pressure vessel failure in high pressure is low due to reliable Automatic Depressurization System (ADS) in BWRs.

Typical ABB Atom BWR containment (Olkiluoto) is shown in Figure 1. The total free volume of the containment is  $\sim 7\,600\text{ m}^3$  (compared to  $\sim 70\,000\text{ m}^3$  in large dry PWR containments), of which  $\sim 4\,500\text{ m}^3$  in the drywell. The containment is divided into compartments by internal structures: the upper drywell, lower drywell (also called as pedestal), and the wetwell including  $2\,700\text{ m}^3$  of water in the suppression pool. The pedestal and the upper drywell are connected with the open flow path having a total area

of 3.8 m<sup>2</sup>. A total of 16 blowdown vent pipes extend vertically from the upper drywell into the suppression pool water. Steam discharging from possible ruptures and leaks in the reactor coolant system is condensed in the pool. The containment is equipped with a filtered venting system to limit the pressure to levels where the containment can preserve its leaktightness. The venting pressure is about 6 bar (abs.), and the design pressure of the containment is 4.7 bar (abs). The containment ultimate pressure limit is about twice the design pressure.

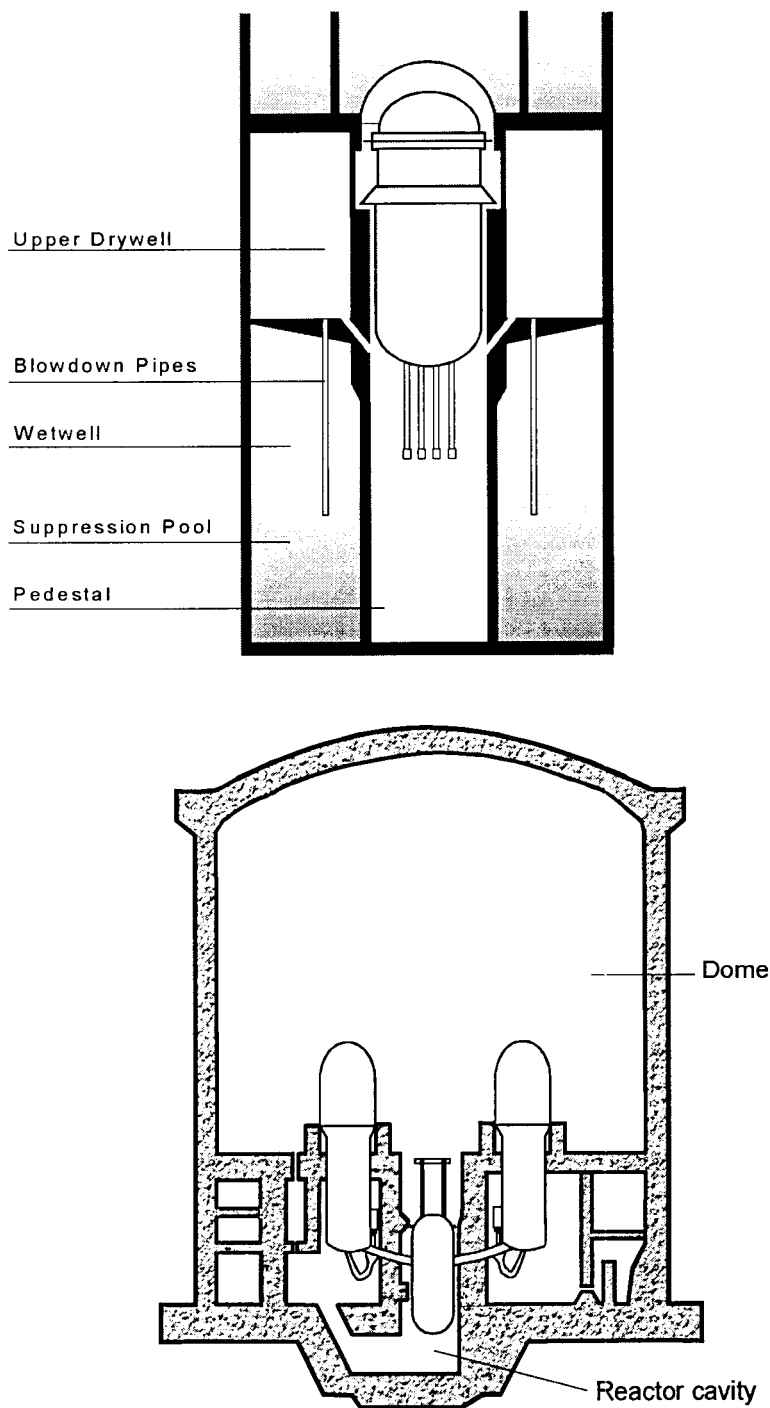


**Figure 1.** A Nordic BWR containment (Olkiluoto) above and a large dry containment (Zion) below. Note that the pictures are not in scale.

The debris dispersal method in BWRs is likely to be different from the DCH scenarios envisaged for PWRs (Figure 1). In a BWR, the vessel will fail most likely from the instrument tube penetration with a small initial hole. We suppose that the discharged melt will be dispersed directly, when entering the relatively large pedestal atmosphere during the first few tens of seconds of the blowdown. This assumption formed the basis for our study. In a PWR, a large amount of melt is assumed to be discharged from the reactor pressure vessel at a pressure that can be twice as high as the normal operation pressure of a BWR. The debris is ejected to the floor in the tight cavity beneath the vessel lower head and the steam/water blowdown following after may entrain and disperse a certain fraction of melt into the upper compartment (dome) atmosphere. The debris transport and dispersion processes are strongly dependent on the containment geometry, the vessel failure pressure, and the lower head failure mode.

The cavity entrainment and the correlations for the dispersed fraction implemented in CONTAIN are validated against the scale experiments performed in typical PWR geometries and conditions only (NEA, 1996). The correlations may not be directly applicable to BWR conditions. In this study, the debris dispersal fraction is therefore parametrically given as a user input.

All Nordic BWR containments are inerted with nitrogen in order to prevent the hydrogen combustion phenomena inside the containment. Regarding to chemical reactions during DCH the inerting also suppresses the most exothermic metal-oxygen reactions.

## 4. TECHNICAL APPROACH

High Pressure Melt Ejection in Olkiluoto BWR was studied numerically by using the CONTAIN 1.2 and MELCOR 1.8.3 computer codes, with CONTAIN being the main tool. Because CONTAIN is purely a containment system code, the strategy was to estimate the debris, steam, and non-condensable gas discharge rates from the pressure vessel to the containment with the MELCOR/BH model and then calculate the containment response with CONTAIN. Also the containment initial conditions at the time of vessel breach defined in the CONTAIN input were based on the MELCOR analyses. For comparison with CONTAIN the stand-alone HPME model in MELCOR was applied to analyse one reference case.

In addition to the BH model calculation, cases were studied, where the ejected core melt was assumed to comprise 15-25 % of the total core material mass with the corium composition being directly proportional to the initial core material inventories (as generally predicted by the MAAP code).

Since many physical and chemical processes involved with HPME and DCH are complicated and modelled only parametrically in the computer codes, a number of parametric variations were calculated with CONTAIN. This was considered necessary to better understand the code behaviour and the dependence of calculational results on the physical and calculational parameters.

## 5. CONTAIN AND MELCOR CODES

CONTAIN is a USNRC's best-estimate containment system code for predicting the physical, chemical, and radiological conditions inside a containment and connected buildings during severe accidents (Murata et al., 1990). Also, models for dominant DCH phenomena have been incorporated in the code (Washington, 1993, Washington & Williams, 1995, Williams & Griffith, 1996). New CONTAIN version 1.2 includes a number of new DCH model improvements described below. The CONTAIN code is modular, and based on the lumped parameter approach.

MELCOR 1.8.3 is a fully integrated engineering-level computer code developed by Sandia National Laboratories for the USNRC, that models the progression of severe accidents in light water nuclear power plants (Summers et al., 1994). MELCOR code includes models for all relevant severe accident phenomena in the primary circuit as well as in the containment, that can be reasonably addressed with lumped-parameter approach (precludes rapid, energetic events and structural analyses).

### 5.1 DCH Models

The CONTAIN DCH model is quite different from the MELCOR FDI/HPME model (Kmetyk, 1993). Generally, CONTAIN uses more mechanistic treatment than MELCOR, which has a simple parametric approach. For example, MELCOR does not handle the intercell debris transport, and the model requires the final debris distribution inside a containment to be given in the input.

#### CONTAIN:

The CONTAIN DCH models cover the following phenomena (Washington & Williams, 1995):

- 1) debris dispersal, debris entrainment, and gas blowdown table options,
- 2) multiple field representation of debris particles,
- 3) debris transport and intercell flows,
- 4) debris trapping,
- 5) chemical metal reactions,
- 6) hydrogen combustion under DCH conditions,
- 7) convective and radiative heat transfer between the debris and atmosphere,
- 8) interactions of non-airborne debris.

The debris ejection and gas blowdown from the RPV is modeled as user-specified input tables. Typically, in PWR geometries, the debris is first specified to be dispersed into the so-called trapped bin in the cavity. Second, the entrainment rate of debris out of the cavity is specified with entrainment input tables. Also specific "candidate" models have recently been added to CONTAIN for predicting the debris ejection, debris dispersal and entrainment from cavity (Williams & Griffith, 1996). These models have been assessed against several experiments performed at Brookhaven National Laboratory and Sandia National Laboratories using Surry and Zion plant cavity geometries.

The CONTAIN DCH model has a multiple field representation of debris particles. Each field can have its own size, mass, chemical composition, and temperature. The debris fields may also have many time groups, called as “generations”, which means that the debris fields can be duplicated any number of times into time groups. This feature allows e.g. the dispersed debris to remain separated from previously dispersed particles.

Debris particles are assumed to flow with gas through interconnecting flow paths. A user-specified slip ratio is used to define the ratio of the velocity of the gas to the velocity of the debris particles.

Complicated trapping processes still include considerable uncertainties and are difficult to model. The CONTAIN trapping rate can be specified by the user or is calculated by the code based on the gas and debris velocities, cell conditions, and particle field parameters. The optional trapping rate models in CONTAIN are

- a) user-specified constant trapping rate,
- b) gravitational fall time of debris particles (GFT),
- c) time to first impact -model (TFI),
- d) time of flight/Kutateladze criterion (TOF/KU)

In the GFT model, the trapping rate (actually settling rate ) is given by a time constant

$$\lambda_{gft} = \frac{v_{gft}}{L_{gft}} \quad (1)$$

where  $v_{gft}$  is the terminal fall velocity of the debris particles, and  $L_{gft}$  is the characteristic gravitational height for debris particle.

In the TFI model, the debris is assumed to strike only one structure and then fall to the floor. The debris flight time to the first structure is calculated by assuming that the debris velocity decreases from the inlet velocity  $v_{d,in}$  to the debris velocity at first impact  $v_{d,1}$  as

$$t_{tfi} = \frac{L_{tfi}}{v_{d,in} - v_{d,1}} \ln \left( \frac{v_{d,in}}{v_{d,1}} \right) \quad (2)$$

where  $L_{tfi}$  is the distance to the first structure. The TFI trapping rate is given by

$$\lambda_{tfi} = \frac{1}{t_{tfi} + t_{gft}} \quad (3)$$

where  $t_{gft}$  is the gravitational fall time.

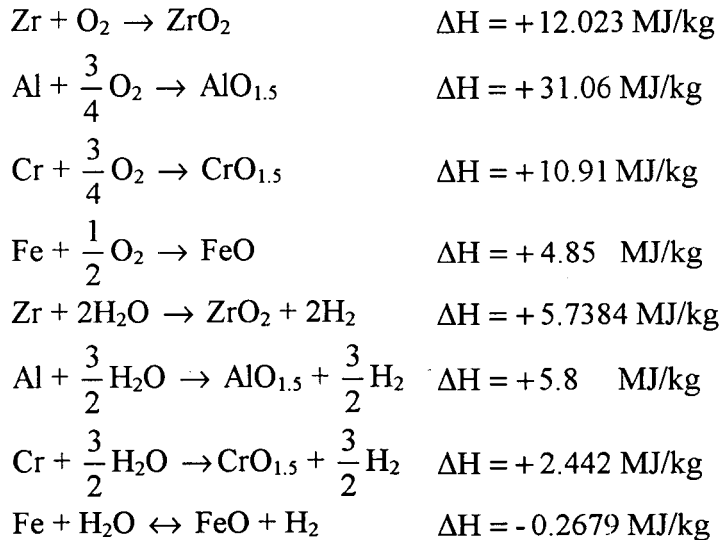
The most mechanistic TOF/KU -trapping model uses a Kutateladze entrainment criterion to determine whether particle re-entrainment occurs after debris has impacted the structure or whether the particles are stucked on the structure surface. The dimensionless Kutateladze number is given by

$$Ku = \frac{\rho_g v_g^2}{\sqrt{(\rho_d - \rho_g)g\sigma}} \quad (4)$$

where  $\rho_d$  is the material density of the debris, and  $\rho_g$  and  $v_g$  are the fluid density and velocity, respectively. When the calculated Kutateladze number is greater than the cutoff value (default 10) the debris is assumed to re-entrain from a surface.

In the TOF/KU trapping model, the particles can stick on the first or the second impact on the structures if the Kutateladze re-entrainment criteria is met. If neither of two re-entrainment criteria are met, the debris particles will either settle gravitationally or flow out of the cell.

The metal components of dispersed debris can react with oxygen and steam releasing chemical energy into cell atmosphere. The following chemical reactions are treated



All metal reactions except for iron/steam are assumed to go to completion.

The chemistry model of CONTAIN includes the modelling of the gas transport to the droplet surface (gas-side transport), the diffusion of oxidant inside the droplet (drop-side transport), the combination of the gas-side and drop-side reaction rates and the hierarchy scheme used to evaluate the amount of metal that reacts in the debris field. Also the recombination of hydrogen produced by the chemical reactions is modeled.

CONTAIN has three models to address hydrogen burning under DCH conditions:

- 1) deflagration
- 2) continuous burning model (diffusion flame)
- 3) spontaneous recombination

The experiments suggest that hydrogen probably does not burn as deflagration under DCH conditions. Continuous burning and spontaneous recombination models are therefore most important in DCH calculations (Gido et al., 1996). In the continuous burning model, the specific fraction of inflow hydrogen is burned in the cell if the user-specified burning criteria are met. The spontaneous recombination model is only a parametrical one, and needs e.g. the recombination rate to be an input parameter.

The models used for the non-airborne debris particles are principally the same used for the airborne ones. Non-airborne debris can, however, have an own user-specified debris diameter.

### MELCOR:

MELCOR 1.8.3 code has a simplified, parametric model for High Pressure Melt Ejection (HPME). The model is invoked in a full plant calculation if the molten debris discharge velocity from the vessel exceeds a user specified value (default= 10 m/s) or the user has chosen the stand-alone mode of the FDI code package by input. The code structure in MELCOR precludes the activation of the BWR specific Bottom Head (BH) Package simultaneously with the FDI package. Hence, if the user wants to use BH package for estimation of the corium composition, temperature and discharge flow rate from the reactor pressure vessel, the most convenient way is to apply the stand-alone mode of the FDI package, as was done in these studies.

The HPME model does not include a mechanistic model for core debris transport, but the user specifies a set of debris destinations and corresponding fractions that prescribe, where the ejected debris is assumed to go (Summers, 1994). The debris destinations can be any control volume atmosphere, heat structure or cavity defined by CAV (CORCON) package. The transport of the debris is assumed to take place instantaneously without any interaction occurring between the discharge location and the defined destination. The transport of debris to heat structures can occur in two ways: first by direct deposition of material on a heat structure as defined by respective transport fraction. This is called trapping in MELCOR, but unlike in CONTAIN, it has no physical modelling in the background. The second mechanism of transport onto heat structures is the settling of particles, determined with the help of user specified input settling time constant, that is used to take into account different settling distances in the control volumes.

The processes that are modeled in the FDI package include oxidation of the metallic components of the debris (Zircaloy, aluminum, steel) in both steam and oxygen, surface deposition of the airborne debris by trapping or settling and heat transfer to the atmosphere and deposition surfaces.

The debris that is defined to be transported into cavity destinations will not be further treated with the FDI package, rather, subsequent treatment is given by CAV package. The cavity model was not invoked in these studies, since core-concrete interaction was not assumed to take place.

The first-order rate equations with user-specified time constants for oxidation, heat transfer and settling are used to determine the rate of each process. The oxidation of the

airborne and deposited debris is only calculated if the debris temperature exceeds a minimum value defined through a sensitivity coefficient (default 600 K). If a water pool exists in the cavity at the time of debris discharge, water is ejected to the atmosphere as droplets (fog) with a rate proportional to the debris ejection rate. The user can change the proportionality constant (default 10), which is strictly parametric and meant for sensitivity analyses only. The size of this parameter may have a strong effect on results.

## 5.2 Main Limitations of the DCH Models

### CONTAIN:

Some key limitations of the CONTAIN DCH model are as follows (Washington & Williams, 1995):

- a) Many trapping processes are not modelled such as surface ablation, drop splashing, film interaction etc.
- b) No mechanistic model for debris water interaction. This also leads to the limitation that no debris particles are allowed to flow through a suppression pool and interact with the water. When the gas flows through the vent pipes from the upper drywell into the suppression pool, debris mass and energy are removed from the upstream cell, but the debris removed from the upstream cell is not placed in the downstream cell (wetwell). Instead, the debris is lost from the problem. In our study, the influence of this limitation on the overall results were supposed to be minor due to very small fraction of debris, which is transported from the upper drywell through the suppression pool vent pipes.
- c) No mechanistic model for debris gas slip.
- d) No mechanistic model for non-airborne debris.
- e) Drop-drop interaction is not modelled.

Many limitations are coupled with a lumped-parameter approach e.g. the debris is only transported by bulk flow between the cells.

### MELCOR:

The key limitations of the MELCOR 1.8.3 model is that the debris transport and trapping are not modeled mechanistically. Specifically, de-coupling the debris transport from the vessel blowdown precludes an accurate investigation of the effects associated with the coherence between the debris and steam ejection. If the loading induced by DCH is primarily limited by the amount of thermal and chemical energy available in the debris, the model can be adequate for parametric PSA studies. However, if the DCH loading is primarily limited by the amount of steam that has an opportunity to interact with airborne debris, the model can underpredict the true DCH threat.

## 6. OLKILUOTO PLANT MODEL

### 6.1 Initial Accident Sequence

The initial accident sequence analysed was a station blackout (TMLB') scenario. The studied accident scenario initiated with the loss of AC and DC power supply. The depressurization of the reactor coolant system was assumed to fail leading to a failure of three instrument tubes in the lower head at full system pressure. The containment studies focused on the short time period (about 120 s) following the instrument tube failure. Most of the critical phenomena occur during the first few tens of seconds after the RPV failure, because the growth of the initial hole in the bottom head leads rapidly to a situation, where the pressure difference is not high enough to disperse the debris directly from the hole. The high pressure melt ejection criteria in MELCOR model is that the debris discharge velocity exceeds 10 m/s and this limit was reached at 20 seconds after the initiation of the blowdown (the RCS pressure at that time was 20 bar).

### 6.2 Reactor Coolant System

The primary system model was the same as in the earlier late phase melt progression studies applying the BH package (Lindholm et al., 1997). Only the number of the lower head penetrations was limited to three instrument tube penetrations to study the effect of a small initial hole. The inner diameter of each instrument tube was 71 mm. The lower head debris bed is divided into three axial layers and into four radial rings taking into account the curvature of the lower head.

The BH package model typically addresses the late lower head penetration failure, when the debris bed in the bottom head is dry. The model assumed that a lower head penetration failure occurred, if the temperature of the debris in a node exceeds the steel melting temperature (1700 K). The molten debris residing above the failure location in the node was assumed to pour into the instrument tube and if the melt does not freeze while flowing down the instrument tube, it is discharged into the pedestal volume.

The initial core material masses in the Olkiluoto reactor were the following:

UO <sub>2</sub>	104 296 kg
Cladding	22 200 kg
Canisters	13 650 kg
Steel	14 719 kg
B <sub>4</sub> C	1258 kg

### 6.3 Containment

#### CONTAIN:

Figure 2 shows the 6-cell containment model used in the CONTAIN analyses. The nodalization and the initial conditions at vessel breach are described in Table 1. The floors and the most significant heat structures were modeled in each cell. Gas region of each cell contained water vapour, three non-condensable gases (H<sub>2</sub>, O<sub>2</sub>, N<sub>2</sub>), and the core debris material. The core concrete interaction and the fission product models were not activated.

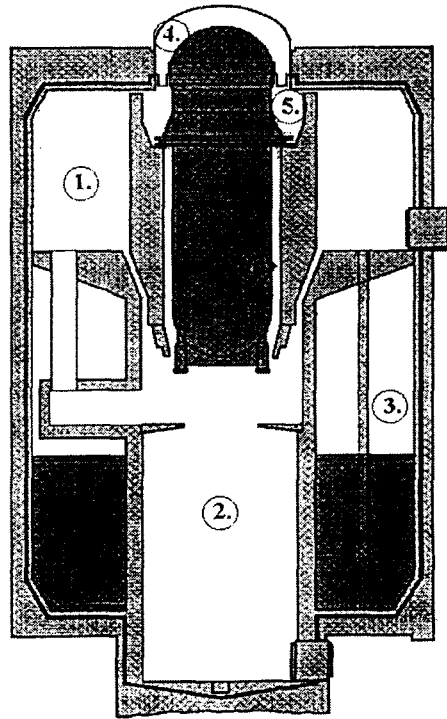


**Figure 2.** Containment nodalization used in the CONTAIN analyses (Keinänen, 1996).

**Table 1.** Containment nodalization and initial conditions used in the CONTAIN analyses.

Cell	Compartment	Free Volume (m <sup>3</sup> )	Initial Pressure (Bar)	Initial Temperature (K)
1	Upper Drywell	2755	2.73	344
2	Pedestal	1300 <sup>*)</sup>	2.73	317
3	Wetwell	3104 <sup>**)</sup>	2.73	368
4	Space Inside the PS-Dome	130	0.97	568
5	Upper Part of Space Inside the Biological Shield	150	2.73	568
6	Lower Part of Space Inside a Biological Shield	171	2.73	568

<sup>\*)</sup> Dry pedestal (no pedestal flooding)

<sup>\*\*)</sup> Initial water mass in the suppression  $2.651 \cdot 10^6$  kg, initial water temperature 349 K

The steam, water, and the debris sources from RPV to the containment were given as input tables. In the cases with the metallic debris source (see section 8), the source data was based on the MELCOR/BH calculation. In the cases using the oxidic debris source, the data is user-specified. Also the steam generation rate simulating steaming from the metal-coolant interaction was specified as user specified input table.

### MELCOR:

The MELCOR containment model for stand-alone application of FDI package was simplified to comprise three containment volumes: pedestal, drywell and wetwell, with floors and walls modeled as heat structures. Key non-condensable gases were defined (N<sub>2</sub>, H<sub>2</sub>, O<sub>2</sub>, CO, CO<sub>2</sub> and CH<sub>4</sub>) as well as the core debris material. No reactor coolant system or core models were active, neither core concrete interaction or fission product models. Figure 3 shows the containment nodalization used for stand-alone HPME analyses.

The blowdown steam source was given as steam mass sources to the pedestal volume. The discharge flow rate of each debris component was given as a tabular function of time through the FDI package input. The temperature of the ejected debris is also defined as a tabular function of time through the FDI package input.

The time constants for oxidation was 0.1 s (value used in the example input in the code manual) and for heat transfer 0.5 s (suggested in the code manual for debris with density being 10000 kg/m<sup>3</sup>, specific heat capacity of 500 J/kg-K and particle diameter of 1 mm). The time constant for debris settling was 0.64 s for pedestal and 1.0 s for drywell. The settling time constant  $t_{\text{settling}}$  was calculated from the formula

$$t_{\text{settling}} = \sqrt{\frac{L}{2 \cdot g}}, \quad (5)$$

where  $L$  is the settling height of the control volume (m), and  $g$  is the constant of gravity (9.81 m/s<sup>2</sup>).

The height of pedestal gas volume was 9.75 m and the height of the drywell volume was 19.4 m. The water pool height in the pedestal was 12.2 m.

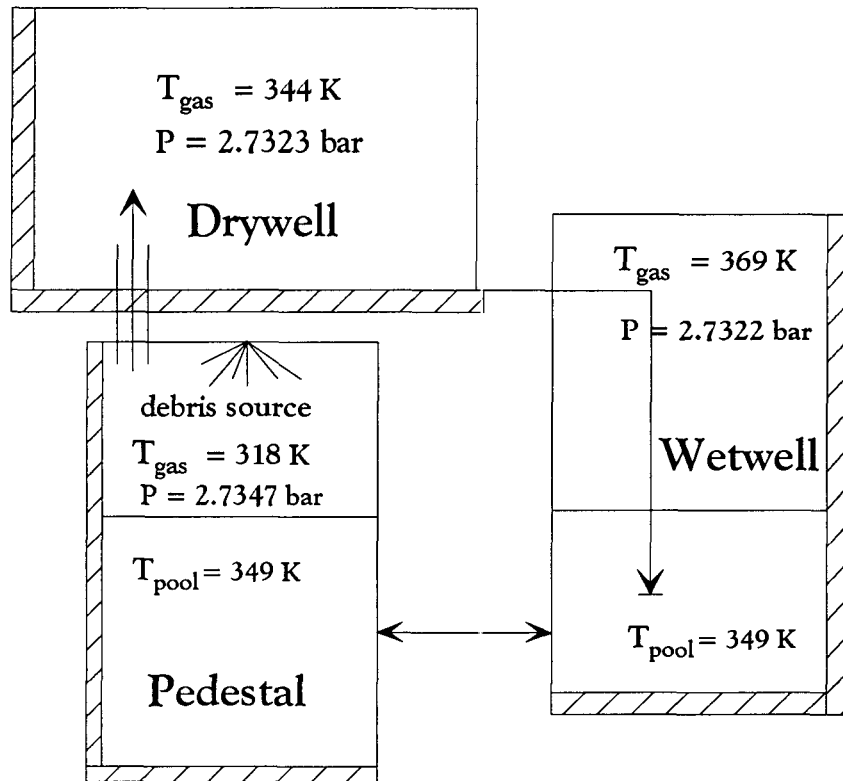


**Figure 3.** *Olkiluoto containment nodalization and initial conditions used in stand-alone HPME calculations with MELCOR.*

In addition to debris mass source, a steam mass source to the pedestal atmosphere was defined to account for the steam released during the blowdown. The steam mass flow rate and temperature were taken from the full Olkiluoto model run with the BH package.

All discharged debris material was assumed to disperse into the containment atmosphere. 80 % of the material was destined to pedestal and 20 % to the drywell atmosphere. Nothing was assumed to be trapped initially on the walls and floors, but the code was allowed to deposit the debris on the pedestal and drywell floor according to the defined settling time.

The initial gas composition in the containment at the vessel breach used in both CONTAIN and MELCOR calculations are shown in Table 2. The values were based on the MELCOR/BH calculation (see section 7).

**Table 2.** *Initial gas composition in the containment at the vessel breach (mol. %).*

Compartment	O <sub>2</sub>	N <sub>2</sub>	H <sub>2</sub>	Vapour
Pedestal	0.4	53.2	38.1	8.3
Upper Drywell	0.14	82.9	15.0	1.96
Wetwell	2.2	14.6	73.3	9.9

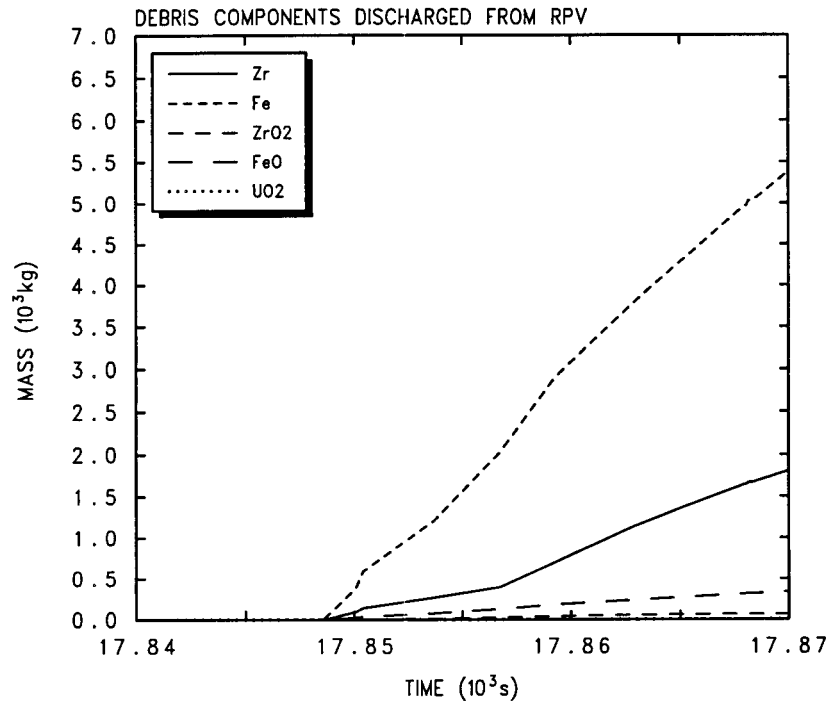
## 7. PRESSURE VESSEL LOWER PLENUM CONDITIONS AT VESSEL BREACH

The accident started with a total loss of electricity. The feedwater injection ceased and the slow boiloff of coolant through the safety relief valves (SRV) commenced leading to core heatup and dryout. The fuel damage started with the cladding failure and release of fission products into the reactor coolant system at 79 minutes into the accident. The core heatup progresses in steam rich atmosphere resulting in high hydrogen generation and releases to the containment through SRVs. Core debris migration into the lower plenum started at 2 h 43 minutes into the accident and was followed by the lower plenum dryout about 1 h later, after which the BH package was immediately initiated. The lower plenum input defined in each radial ring one instrument tube penetration having an inner diameter of 71 mm. The temperature of the lower head debris bed increased and reached the failure temperature of the instrument tubes in the second axial layer, almost simultaneously in all three radial rings at 5 h into the accident. When an instrument tube fails, the model allows only the molten material residing above the failure location (in this case in axial layers 2 and 3) pour into the instrument tube channel.

At the time of instrument tube failure about 30 000 kg of material in the layer 2 was in molten state corresponding to a melt fraction of 30 % of the total layer 2 debris mass. The average debris temperature in the layer 2 was 1675 K. The melt fraction of the other debris layers was negligible. The reactor coolant system pressure dropped below 20 bars in 20.2 seconds after the instrument tube failure. The pressure of 20 bar was used as the cut off pressure for the high pressure melt ejection. The hole size grew rapidly; according to performed scoping studies with MELCOR, the hole would be three times its original size in about 10 seconds. These two facts supported the decision made in these analyses, that debris jet will not be dispersed, when the pressure difference between the lower plenum and the containment is below 20 bar.

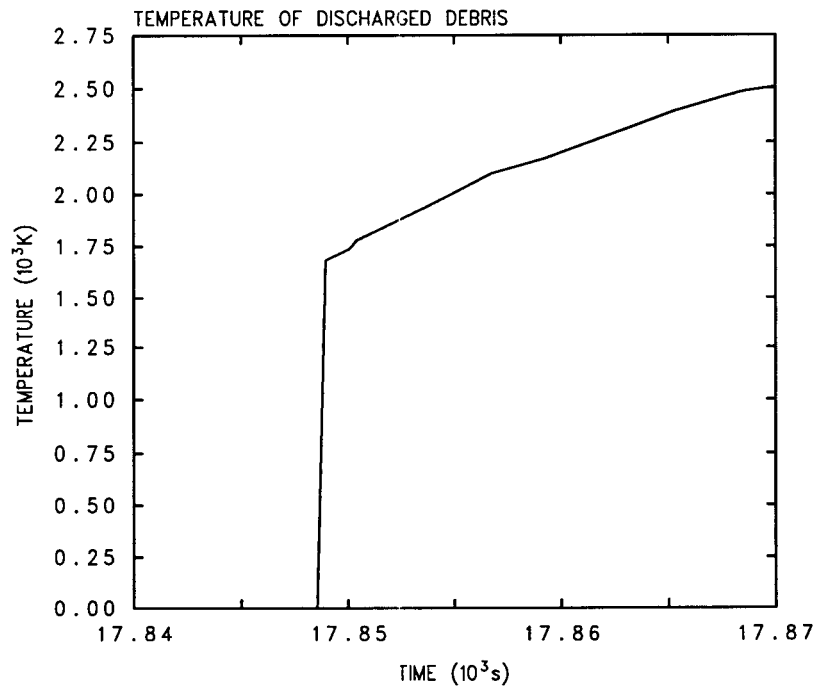
A total amount of ~ 9800 kg of debris was ejected during a period of 20.2 seconds. Figures 4 and 5 show the cumulative discharged debris mass by components and the temperature of the discharged debris, respectively. The steam mass discharged during the blowdown is shown in Figure 6. The temperature of discharged steam was taken to be equal to the steam temperature in the lower plenum atmosphere, i.e. 1000 - 1250 K. The steam in the pressure vessel was highly superheated due to heat transfer from the debris upper surface and from the hot upper plenum structures.

When the instrument tubes failed the debris temperature was relatively low and the melt consisted mostly of metals. This is a result from the core relocation pattern from the core region to the lower plenum. In these calculations, the debris drained into the lower head water pool and was assumed to be fragmented and quenched. The remelting of debris occurred by components.



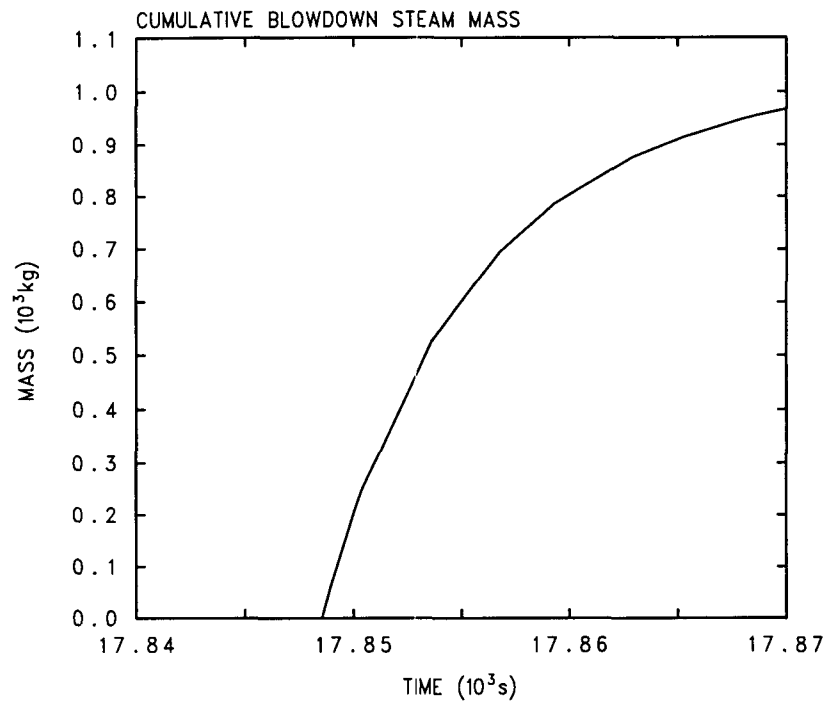
High pressure case, BH model active, No FDI model

**Figure 4.** Discharged debris mass by components.



High pressure case, BH model active, No FDI model

**Figure 5.** Temperature of debris ejected from the RPV.



High pressure case, BH model active, No FDI model

**Figure 6.** *Cumulative mass of steam discharged from the RPV to the pedestal.*

## 8. CONTAINMENT RESPONSE

The containment analyses were divided into two categories according to the composition of discharged debris: metallic and oxidic debris cases. In the base case with the metallic debris, all sources from the reactor coolant system to the containment were based on the MELCOR/BH calculation as described in section 7. In the base case with the oxidic debris, the source data was specified assuming that ~ 25 % of the whole core material inventory and 34 000 kg of saturated water was discharged from RPV during 30 seconds. 60% (~ 22 500 kg) of the discharged debris is assumed to disperse directly to the pedestal atmosphere. The rest of the debris is directed to the pedestal water pool. In this case, the debris consisted mostly of oxides. Characteristics of the sources in both base cases are summarized in Table 3.

**Table 3.** Sources from the reactor coolant system to containment at vessel breach, base cases with the metallic and oxidic debris sources.

Case	Dispersed Debris Mass (kg)	Debris Temperature (K)	Melt Composition (%)					Discharged Water, Saturated (kg)	Discharged Steam, Superheated (kg)
			Zr	Fe	Feo	ZrO <sub>2</sub>	UO <sub>2</sub>		
Metallic Debris	~ 10 000	1 700 - 2 500	19.1	76.6	3.6	0.7	10 <sup>-3</sup>	-	~ 1 000 *)
Oxidic Debris	22 500	2 500	16	10	-	7	67	34 000 **)	-

\*) Steam temperature 1000-1250 K

\*\*) Saturation temperature corresponding the full reactor coolant system pressure of 70 bar.

### 8.1 Metallic Debris Source

#### 8.1.1 Code Benchmark Case

Although CONTAIN was the main tool in the containment analyses, the containment response was calculated in one reference case both with MELCOR and CONTAIN comparing the MELCOR capabilities against more detailed CONTAIN code. The application of the simple MELCOR model is justified by the fact that the code is currently the main tool for integral severe accident calculations for Olkiluoto NPP.

In the comparison case, the pedestal was assumed to be dry. Thus, no pedestal flooding from the suppression pool was modelled. The debris discharge and blowdown source data from RPV was extracted for CONTAIN from the MELCOR/BH analysis described in section 7. The melt consisted mostly (about 96%) of metals.

The key boundary conditions e.g. the debris and blowdown discharge data, and the containment initial conditions were consistently specified for both codes. However, some input differences inevitably remained due to unique features of the codes' DCH models.

In the simple HPME calculation with stand-alone version of FDI package in MELCOR 1.8.3, the discharged debris was assumed to disperse totally to the containment

atmosphere, so that 80 % of the debris was destined to the pedestal atmosphere and 20 % to the drywell atmosphere. In the CONTAIN calculation, all debris material was initially assumed to disperse to the pedestal atmosphere. CONTAIN further calculated the intercell flow of debris from the pedestal to the upper drywell based on the gas velocity and the user-specified gas-debris slip factor.

The debris particle diameter was assumed to be 1.0 mm in the CONTAIN calculation corresponding to the value used in MELCOR to evaluate important time constants for e.g. oxidation, heat transfer, and droplet settling. The DCH chemistry model of CONTAIN includes both the gas-side and drop-side transport models. In order to be conservative, the drop-side transport limitation was bypassed by setting the drop-side diffusivity to infinity.

The containment pressure responses are shown in Figure 7. The calculated pressure peaks were ~ 7 - 8 bar. MELCOR predicted ~ 1 bar higher pressure maximum than CONTAIN.

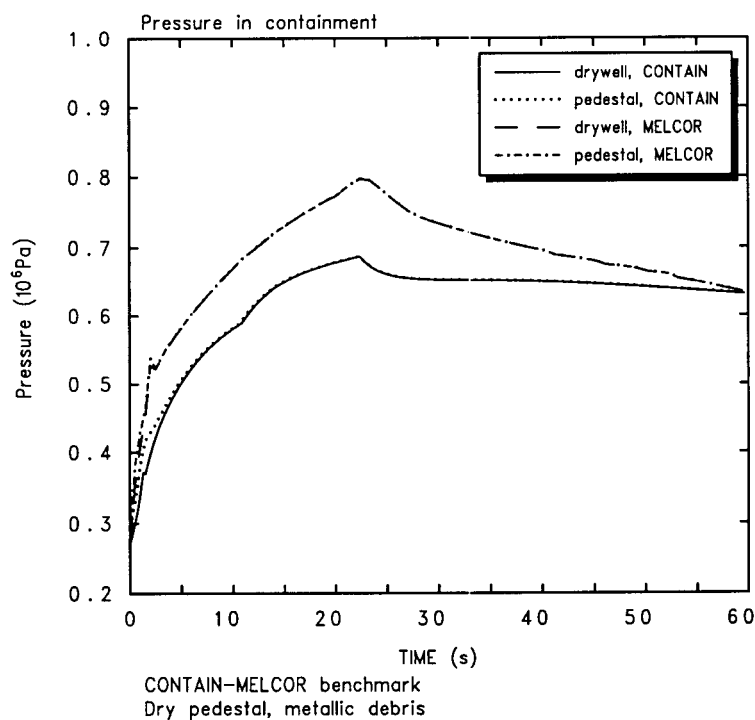


**Figure 7.** Pressure in the pedestal. MELCOR-CONTAIN comparison case. Metallic debris.

The gas temperatures in the pedestal and the drywell behaved differently (Fig. 8). The maximum gas temperature in the pedestal was about 1900 K with CONTAIN predicting ~ 400 K higher values than MELCOR. The gas temperature maximum in the upper drywell was ~ 1400 K, higher value predicted now with MELCOR. Very high gas temperatures were consequences of the release of highly superheated steam from the RPV and of the heat release from oxidation of metallic debris particles. Despite the conservative assumption used in the CONTAIN calculation (infinite drop-side diffusivity), MELCOR predicted more complete and intensive chemical reactions than

CONTAIN. MELCOR estimated ~ 350 kg hydrogen production during the debris discharge. Corresponding CONTAIN estimate was ~ 165 kg.

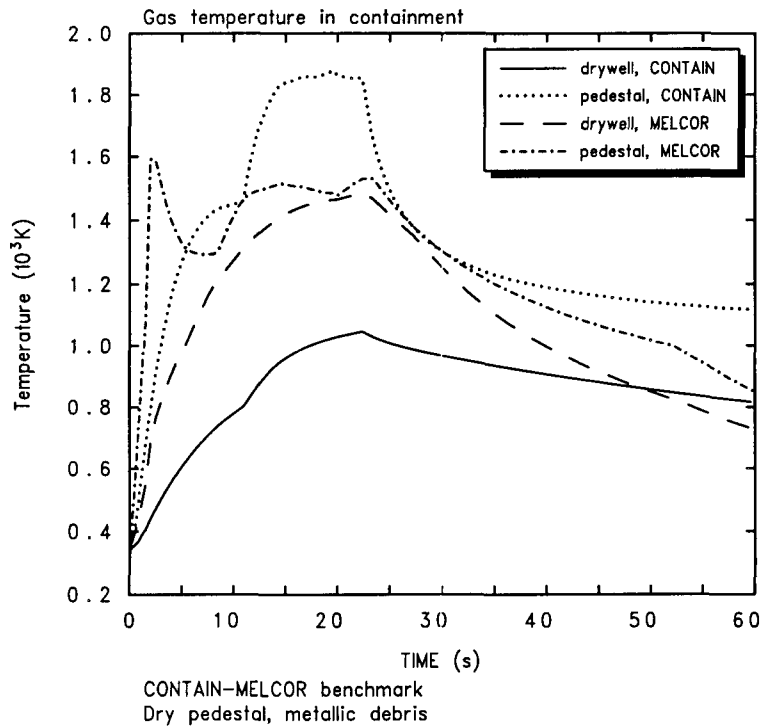


**Figure 8.** Gas temperatures in containment. MELCOR-CONTAIN comparison case. Metallic debris.

The airborne corium masses in the pedestal and drywell atmospheres are shown in Fig. 9. The debris is rapidly settled once released to containment. In the MELCOR prediction, a first order rate equation with a user specified time constant for settling was used. For comparison, a simple removal model based on the gravitational falling of the debris particles was used in CONTAIN, which was assumed to be the most consistent model with the MELCOR time constant method.

As seen in Figure 9, the MELCOR and CONTAIN calculations were in relatively good agreement with the airborne debris masses in pedestal. However, MELCOR predicted a clearly higher debris mass in the upper drywell. This is due to the limitation of MELCOR in modelling the intercell transport of the airborne debris. The consequence is that the user must specify a set of debris destinations and corresponding fractions that prescribe, where the ejected debris is assumed to go. In the MELCOR calculation, 20% of hot debris was directly ejected to the upper drywell atmosphere, whereas in the CONTAIN calculation, most of the debris particles (~ 95%) were trapped and deposited in the pedestal. The rest of the particles were cooled in the pedestal atmosphere prior to flowing to the upper drywell.

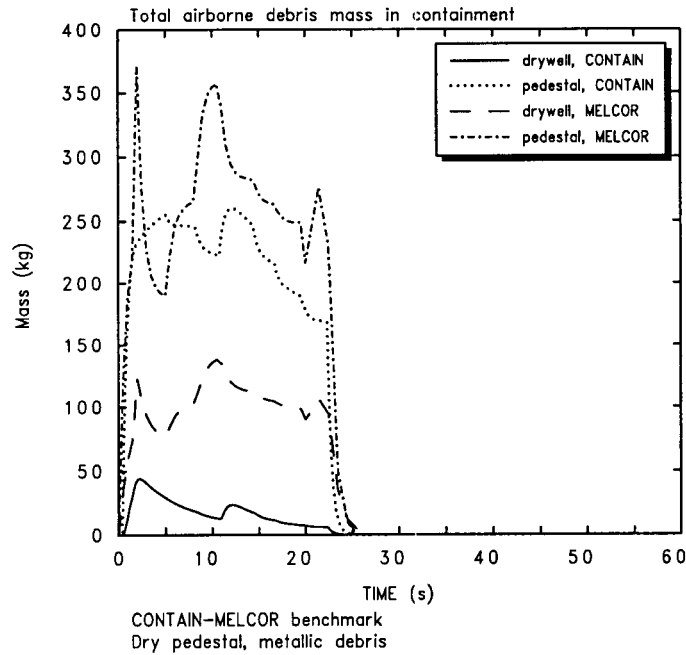


**Figure 9.** Airborne debris masses in containment. MELCOR-CONTAIN comparison case. Metallic debris

### 8.1.2 Sensitivity Calculations

Lumped parameter codes, like MELCOR and CONTAIN, have inherent limitations in modelling the rapid and highly geometry dependent DCH phenomena. The models consist of several correlations to describe DCH phenomena with a set of user specified sensitivity parameters. Regarding to CONTAIN-MELCOR comparison case with the metallic debris, additional sensitivity analyses were performed with CONTAIN varying certain physical boundary conditions and some key model parameters like droplet diffusivity and particle size.

In the CONTAIN-MELCOR comparison case, CONTAIN assumed instant drop-side oxidation reactions due to infinite drop-side diffusivity used. In reality, the reaction rates may, however, be limited by mass transport within the debris particles. Some estimates for drop-side diffusivities are given in the reference (Williams et al., 1987) based upon investigations by Baker and Power et al. (Baker, 1986, Powers et al., 1986). In these estimates the diffusivity was assumed to be in order of  $10^{-8}$  m<sup>2</sup>/s in temperature range of ~ 2000-2500 K, which is also the CONTAIN default value. The value  $10^{-8}$  m<sup>2</sup>/s was therefore selected as diffusivity for the base case calculation. Other assumptions used in the base case calculation were as follows:

- a) dispersed debris mass ~ 10 000 kg,
- b) debris discharge time 22 seconds,
- c) drop-side diffusivity of  $10^{-8}$  m<sup>2</sup>/s,
- d) particle diameter of 1.0 mm,
- e) dry pedestal (no flooding),
- f) “trapping” (settling) of the debris particles by gravitational falling.

The main results of the sensitivity analyses are summarized in Table 4 including the maximum pressure in the pedestal, maximum gas temperature in the pedestal and the upper drywell, and the total amount of hydrogen produced by the chemical metal-steam reactions during the debris discharge.

**Table 4.** Summary of CONTAIN sensitivity study, metallic debris case.

Case	Main Characteristics	P <sub>max</sub> (bar)	T <sub>max</sub> Pedestal (K)	T <sub>max</sub> Drywell (K)	H2 Production (kg)
A1	Base Case	6.8	1790	1028	103
A2 <sup>*)</sup>	Infinite Drop-side diffusivity	6.8	1855	1037	170
A3	Drop-side diffusivity 10 <sup>-10</sup> m <sup>2</sup> /s	6.2	1347	823	5.5
A4	Particle diameter 0.5 mm	~ 7.1	~ 2000	~ 1100	~ 215
A5	Particle diameter 5.0 mm	5.7	996	669	6.5
A6 <sup>**)</sup>	Particle diameter 0.1-5.0 mm	6.8	1691	1033	149
A7 <sup>***)</sup>	Flooded pedestal, no steam generation from pedestal pool	7.6	1912	1071	103
A8	Flooded pedestal, 200 kg/s steam generation from pedestal pool	8.7	1432	1124	117
A9	TOFKU trapping modelling	6.7	1758	985	92
A10	No trapping in pedestal	7.3	~ 1950	~ 1300	~ 177
A11	Dispersed debris mass 22 500 kg	~ 7.1	~ 2000	~ 1100	~ 220

<sup>\*)</sup> CONTAIN-MELCOR comparison case

<sup>\*\*)</sup> Rectangular particles size distribution (five size classes: 0.1, 0.5, 1.0, 2.0, and 5.0 mm)

<sup>\*\*\*)</sup> No steam generation from melt-water interaction

The highest pressure maximum ~ 8.7 bar was predicted in case A8 where the pedestal was flooded with water prior to the vessel breach, and a constant steam generation rate of 200 kg/s was assumed to follow the debris-water interaction. One should remember, that CONTAIN can not mechanistically model melt-water interaction and the following steam generation. The steaming rate was roughly scaled to be proportional to the steam production rates obtained in the FARO experiments (Magallon, D. & Hohman, H., 1993, Magallon, D. et. al. 1997) assuming that ~ 15% of the melt energy was transferred for steam generation.

About 1 bar higher pressure was predicted in the flooded-pedestal case (A7) than in dry-pedestal case (A1), if no steam generation was assumed to occur from metal-coolant interaction. In reality, the pressurization in the wet-pedestal case is also dependent on the steaming rate due to the melt-coolant interaction. The predicted pressure maximum ranged about 1.5 bar in all dry-pedestal cases analysed (from 5.7 to 7.3 bar). The sensitivity to drop-side diffusivity (metal oxidation) can be seen in cases A1, A2, and A3. Case A2 in which an infinite drop-side diffusivity was used yielded the most intensive chemical reactions and highest gas temperatures of the three cases above. The drop-side diffusivity of 10<sup>-10</sup> m<sup>2</sup>/s (Case A3) was small enough to suppress all chemical reactions (only about 5 kg hydrogen was generated).

The sensitivity to particle size was studied with three different particle diameters: 0.5, 1.0, and 5.0 mm (cases A4, A1, A5). In addition, in case A6, a rectangular distribution ranging from 0.1 to 5.0 mm was used for the particle size. The increase of the particle size from 0.5 to 5.0 mm reduced the maximum pressure from 7.1 to 5.7 bar. Correspondingly, the maximum gas temperature in the pedestal was reduced from ~ 2000 to 996 K.

The influence of different trapping models can be compared in cases A1, A9, and A10. The most “mechanistic” trapping model based on the Kutateladze entrainment criterion (A9) resulted in the most rapid particle removal from the containment atmosphere leading to the lowest pressure and temperature maximum of the three cases. In case A10, the particle trapping (and settling) was totally prevented in the pedestal. This very conservative assumption lead to the longest “flying” time of the airborne particles and to higher containment pressure and temperatures than observed with the other trapping options.

In case A11, the dispersed debris mass was doubled compared to base case A1 (22 500 kg versus ~10 000 kg). The influence on the maximum pressure was minor. The doubled debris source resulted in ~ 100-200 K higher gas temperature than the base case.

There was not sufficient steam in the containment to oxidize all of the metal components of the debris. The initial steam mass in the pedestal and upper drywell was ~ 400 kg. In addition, 1000 kg superheated steam was released from RPV during the debris discharge. Totally ~ 2000 kg of steam would be needed for complete oxidation. In base case A1, about 96% of Zr and 10% of Fe was oxidized at the end of the melt ejection.

Containment pressure histories in the pedestal in cases A1, A2, A3, A5, A6 and A7 are shown in Figure 10 including the sensitivity to droplet size, drop-side diffusivity and pedestal flooding.

Corresponding gas temperatures in the pedestal and the drywell are plotted in Figures 11 and 12, respectively. The gas temperatures were very sensitive to model parameters, especially in the pedestal, where the predicted temperature maximum ranged from ~ 1000 K to 1900 K depending on the used model parameters.

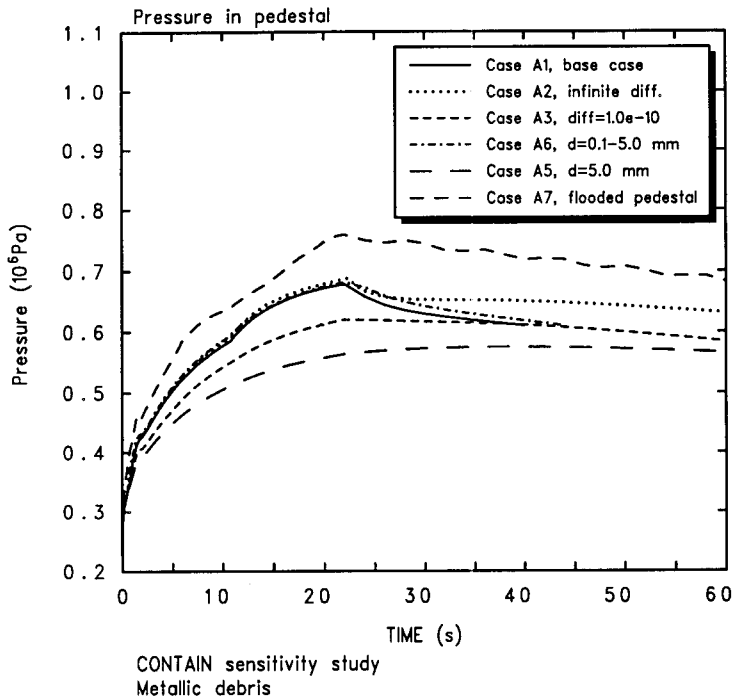


**Figure 10.** Containment pressure histories in the pedestal predicted by CONTAIN. Sensitivity to particle size, drop-side diffusivity, and pedestal flooding. Metallic debris.

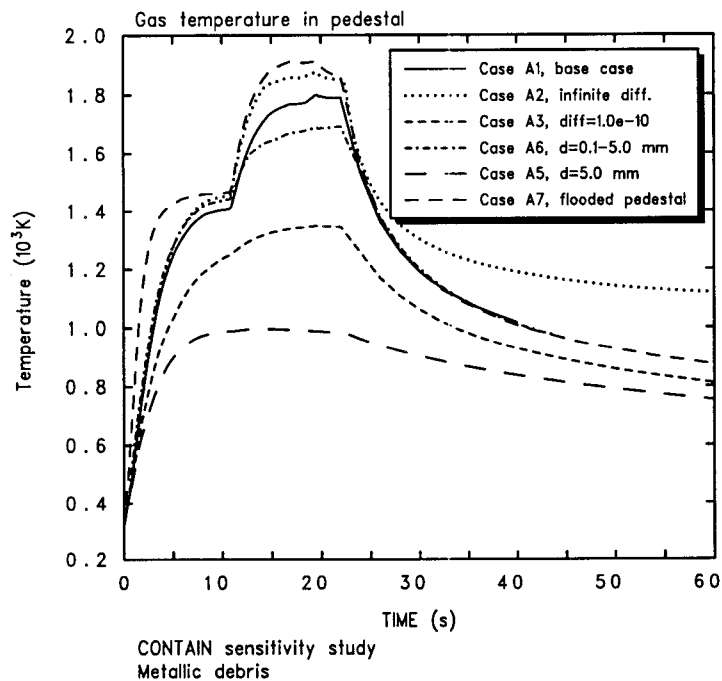


**Figure 11.** Gas temperature histories in the pedestal predicted by CONTAIN. Sensitivity to particle size, drop-side diffusivity, and pedestal flooding. Metallic debris

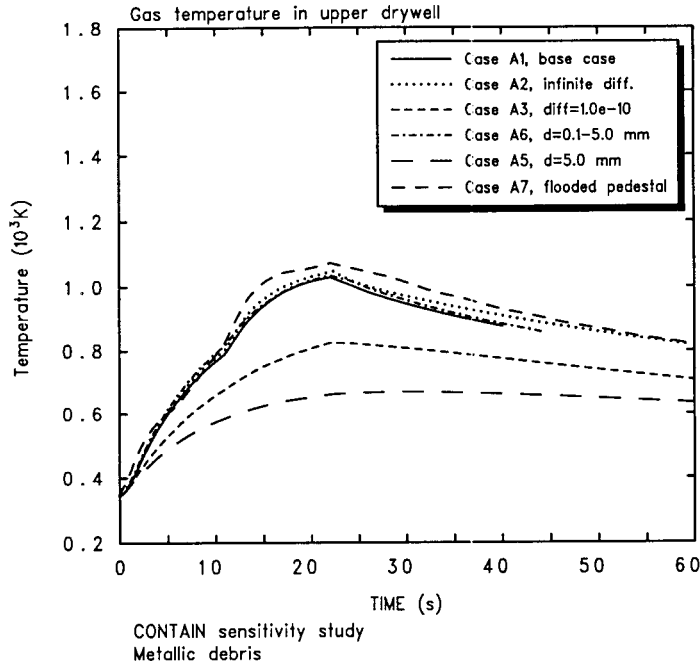


**Figure 12.** Gas temperature histories in the drywell predicted by CONTAIN. Sensitivity to particle size, drop-side diffusivity, and pedestal flooding. Metallic debris

## 8.2 Oxidic Debris Source

If a large mass of debris would rapidly pour into the lower head, the debris might not quench and a melt pool would form into the lower head. In this case, the melt temperatures would be higher containing also liquid oxides. This case would be an example of early instrument tube failure. This scenario with selected sensitivity analyses were addressed with CONTAIN, by assuming ad hoc that ~ 25 % (38 700 kg) of the whole core material inventory and 34 000 kg of saturated water were discharged from RPV during 30 seconds. 60% (~ 22 500 kg) of the discharged debris is assumed to disperse directly to the pedestal atmosphere. The rest of the debris is directed to the pedestal water pool. Steam generation as a consequence of the melt-coolant interaction was simulated by incorporating a constant steam mass flow rate of 300 kg/s to the pedestal atmosphere during the first 30 seconds of the calculation. The steaming rate was roughly scaled from FARO test data to appropriate values to Olkiluoto plant case (Magallon, D. & Hohman, H., 1993). The melt composition was determined on the basis of the material mass fractions of an intact core and the melt was assumed to be at the temperature of 2500 K. The discharged debris consisted mostly (77%) of oxides.

The following assumptions were used in the base case calculation with the oxidic debris:

- a) dispersed debris mass 22 500 kg,
- b) debris discharge time 30 seconds,
- c) drop-side diffusivity of  $10^{-8} \text{m}^2/\text{s}$ ,
- d) particle size of 1.0 mm,
- e) wet (flooded) pedestal,
- f) steam generation rate from the pedestal water pool of 300 kg/s (simulating the steam generation from melt-coolant interaction),
- g) “trapping” (settling) of the debris particles by gravitational falling.

The summary of the CONTAIN results using the oxidic debris source is listed in Table 5.

**Table 5.** Summary of CONTAIN sensitivity analyses, oxidic debris case.

Case	Main Characteristics	P <sub>max</sub> (bar)	T <sub>max</sub> Pedestal (K)	T <sub>max</sub> Drywell (K)	H2 Production (kg)
B1	Base Case	7.4	464	486	88
B2	Infinite Drop-side diffusivity	7.7	463	489	176
B3	Particle diameter 0.5 mm	7.3	446	463	57
B4	Particle diameter 5.0 mm	6.5	439	494	6
B5 <sup>*)</sup>	Particle diameter 0.1-5.0 mm	7.1	446	462	40
B6	Gas/debris slip = 5.0	7.4	467	454	90
B7	TOFKU trapping modelling	7.4	446	467	81
B8 <sup>**)</sup>	Metallic debris: 75% Fe, 20% Zr, 4% FeO, 1% ZrO <sub>2</sub>	8.6	480	510	306
B9	Dispersed debris mass 38 717 kg	8.1	481	509	153
B10	Debris discharge time 22 seconds	7.6	472	499	88

<sup>\*)</sup> Rectangular particles size distribution (five size classes: 0.1, 0.5, 1.0, 2.0, and 5.0 mm)

<sup>\*\*)</sup> The debris composition approximately corresponds the melt composition used in the

CONTAIN-MELCOR comparison case and related sensitivity analyses in section 8.1. Generally, the pressures of the oxidic debris scenarios were relatively insensitive to parametric variations. Only case B8 in which the debris composition was highly metallic, and case B9 in which very big debris mass (38 700 kg) was assumed to disperse to the pedestal atmosphere, yielded over 8 bar pressure maximum. The lowest pressurization was predicted with a large particle diameter of 5.0 mm (Case B4).

The gas temperatures were insensitive to model parameters, and significantly lower than in the metallic debris scenarios described in sections 8.1.1 and 8.1.2. The explanation for that is the “cooling” effect of steam, which is produced in the oxidic debris scenario by flashing of the saturated water assumed to be released coherently with the debris from RPV. A large amount of saturated steam released determined the containment gas temperature, not the DCH heating processes, and hence the influence of model parameter variations is minor.

The blowdown water flashing produced sufficiently steam to oxidate the metal components of the debris. However, the low gas temperatures decreased the chemical

reaction rate, and only 60% of Zr was oxidized in base case B1 at the end of the melt ejection. No oxidation of Fe was observed.

Containment pressure histories in the pedestal in cases B1, B2, B3, B4, B5 and A7 are shown in Figure 13 including the sensitivity to droplet size, drop-side diffusivity and debris composition.

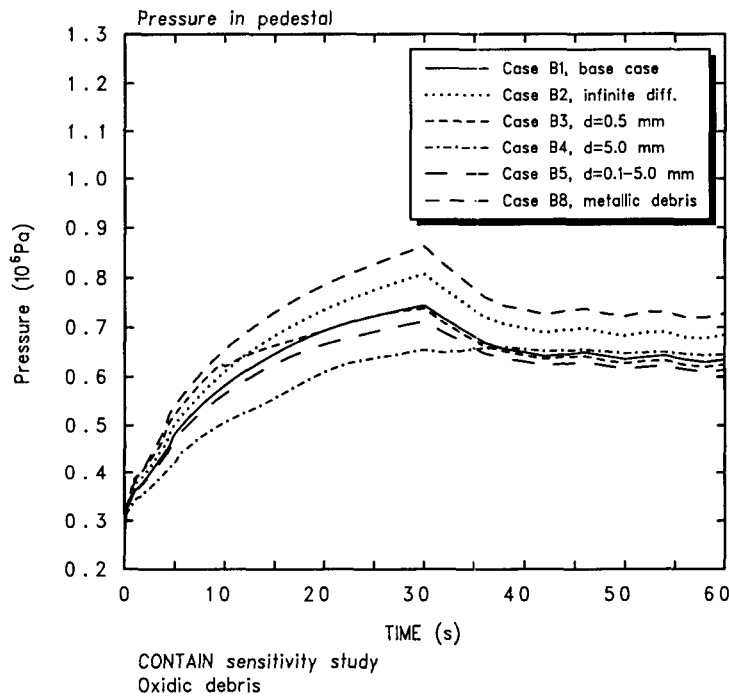


**Figure 13.** *Containment pressure histories in the pedestal predicted by CONTAIN. Sensitivity to particle size, drop-side diffusivity, and debris composition. Oxidic debris base case.*

Corresponding gas temperatures in the pedestal and the drywell are plotted in Figures 14 and 15, respectively. The sudden jump in the drywell gas temperatures at  $t = 30$  s is due to assumed interruption of the blowdown water discharge from RPV. After the flashing of saturated water ceased (steam generation stopped) there are still hot airborne debris particles in the pedestal warming the atmosphere. The temperature increase stopped when the last particles were cooled or removed from the pedestal atmosphere.

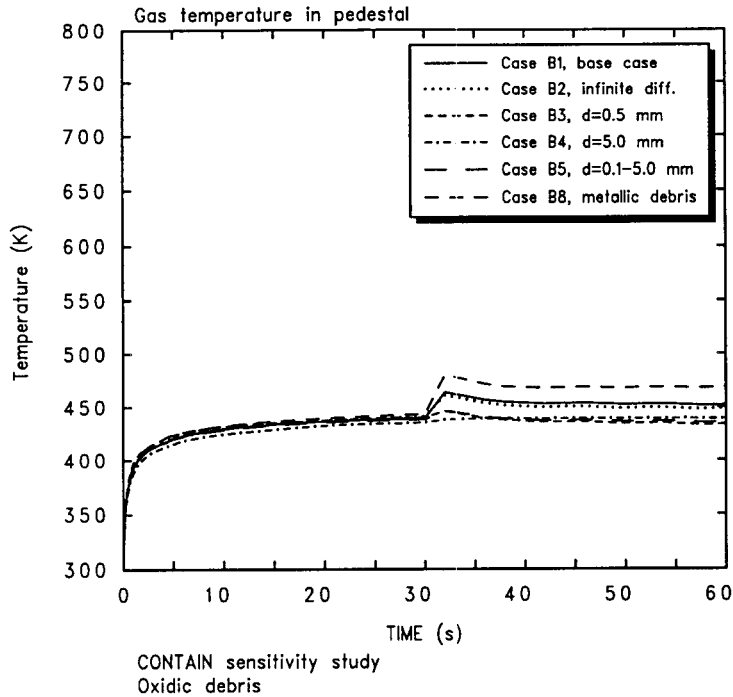


**Figure 14.** Gas temperature histories in the pedestal predicted by CONTAIN. Sensitivity to particle size, drop-side diffusivity, and melt composition. Oxidic debris base case.

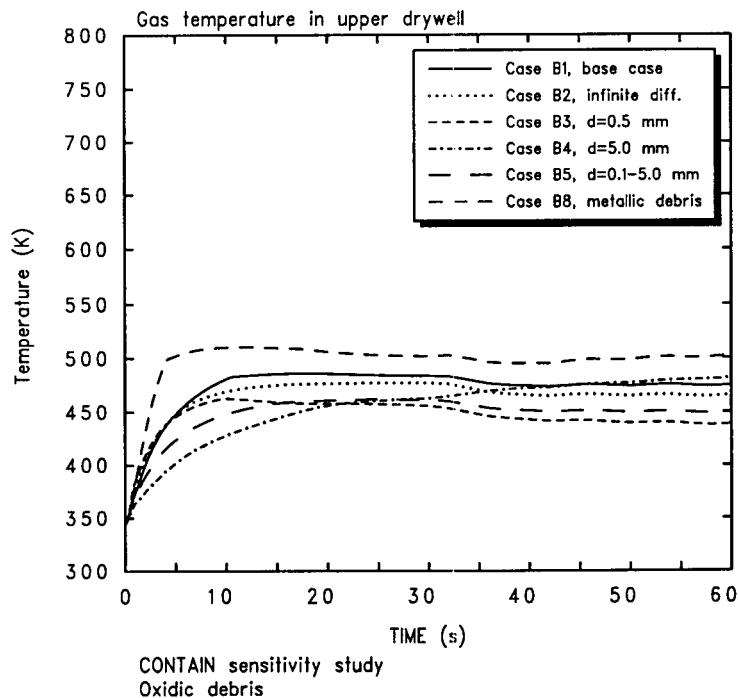


**Figure 15.** Gas temperature histories in the drywell predicted by CONTAIN. Sensitivity to particle size, drop-side diffusivity, and melt composition. Oxidic debris base case.

## 9. CONCLUSIONS

The containment thermal hydraulic loads during high pressure melt ejection in a ABB Atom BWR were parametrically studied with the CONTAIN and MELCOR codes.

The highest calculated pressure peaks were about 8.5 bar. In the scenarios with highly metallic debris source, very high gas temperatures of about 1900 K were predicted in the pedestal, and about 1400 K in the upper drywell. The high temperatures were consequences of the highly superheated steam released simultaneously with debris from the reactor pressure vessel, and of the heat released from oxidation of metallic debris particles. The calculations with metallic debris were sensitive to model parameters, like the particle size and parameters, which control the chemical reaction kinetics.

In the scenarios having an oxidic debris source, the predicted pressure peaks were comparable to the cases with the metallic debris source. The maximum gas temperatures (about 450-500 K) in the containment were, however, significantly lower than in the respective metallic debris case. The temperatures were also insensitive to parametric variations. This can be explained by the cooling effect of steam, which is produced in the oxidic debris scenario by flashing of the saturated blowdown water. The containment gas temperature was determined by the large amount of saturated steam, not by the Direct Containment Heating processes. Due to minor effect of DCH on the containment temperature loads, the influence of model parameter variations was insignificant.

Although CONTAIN was the main tool in the containment analyses, one containment calculation was performed with the MELCOR code for benchmarking of the MELCOR capabilities against more detailed CONTAIN code. In the comparison case, MELCOR predicted ~ 1.5 bar higher pressure maximum than CONTAIN (8 versus 6.5 bar). The predicted gas temperatures also behaved differently. One reason for that was the limitation of MELCOR in modelling the intercell transport of the airborne debris. The user must specify a set of debris destinations and corresponding fractions that prescribe, where the ejected debris is assumed to go. In the CONTAIN calculation, most of the debris particles (~ 95%) were trapped and deposited in the pedestal. The rest of the particles were cooled in the pedestal atmosphere prior to flowing to the upper drywell. Despite the conservative assumption used in the CONTAIN calculation (infinite drop-side diffusivity), MELCOR predicted more complete and intensive chemical reactions than CONTAIN. MELCOR estimated ~ 350 kg hydrogen production during the debris discharge. Corresponding CONTAIN estimate was ~ 165 kg.

The CONTAIN DCH model is more mechanistic than the MELCOR FDI/HPME DCH model, which has a fully parametric approach. CONTAIN is therefore recommended as a best-estimate code for DCH containment analyses. However, if the loading induced by DCH is primarily limited by the amount of thermal and chemical energy available in the debris, also the MELCOR/FDI model can be adequate.

The calculations showed that if a high pressure melt ejection occurred during a severe accident, it could jeopardize leaktightness of the upper drywell penetrations due to high temperature loads. Another consequence would be an early containment venting.

## 10. REFERENCES

- Allen, M.D., Pilch, M., Griffith, R.O., Williams, D.C., and Nichols, R.T., 1992a. The Third Integral Effects Test (IET3) in the Surtsey Test Facility. SAND92-0166, Sandia National Laboratories, Albuquerque, NM. March 1992.
- Allen, M.D., Blanchat, T.K., Pilch, M., and Nichols, R.T., 1992b. Results of an Experiment in a Zion-like Geometry to Investigate the Effect of Water on the Containment Basement Floor on Direct Containment Heating (DCH) in the Surtsey Test Facility: The IET-4 Test. SAND92-1241, Sandia National Laboratories, Albuquerque, NM.
- Allen, M.D., Blanchat, T.K., Pilch, M., and Nichols, R.T., 1992c. Experimental Results of an Integral Effects Test in a Zion-like Geometry to Investigate the Effect of a Classically Inert Atmosphere on Direct Containment Heating: The IET-5 Experiment. SAND92-1623, Sandia National Laboratories, Albuquerque, NM. Nov. 1992.
- Allen, M.D., Blanchat, T.K., Pilch, M., and Nichols, R.T., 1993a. An Integral Effect Test in a Zion-like Geometry to Investigate the Effect of Pre-Existing Hydrogen on Direct Containment Heating in the Surtsey Test Facility: The IET-6 Experiment. SAND92-1802, Sandia National Laboratories, Albuquerque, NM. Jan. 1993.
- Allen, M.D., Blanchat, T.K., Pilch, M., and Nichols, R.T., 1993b. An Integral Effect Test to Investigate the Effect of Condensate Levels of Water and Preexisting Hydrogen on Direct Containment Heating in the Surtsey Test Facility: The IET-7 Experiment. SAND92-2021, Sandia National Laboratories, Albuquerque, NM. Jan. 1993.
- Allen, M.D., et al., 1994. Experiments to Investigate Direct Containment Heating Phenomena with Scaled Models of the Zion Nuclear Power Plant in the SURTSEY Test Facility. Sandia National Laboratories, SAND93-1049, NUREG/CR-6044.
- Baker, L., 1986. Droplet Heat Transfer and Chemical Reactions During Direct Containment Heating, in Proceeding of the International ANS/ENS Topical Meeting on Thermal Reactor Safety. San Diego, CA, February 2-6, 1986.
- Thomas K., Blanchat, and Michael D. Allen, 1995. Experiments to Investigate DCH Phenomena with Large-Scale Models of the Zion and Surry Nuclear Power Plant. Nuclear Engineering and Design. Volume 164(1996) Nos. 1-3. August I 1996.
- Fontana, M.H., 1993. Recent Advances in Severe Accident Technology - Direct Containment Heating in Advanced Light Water Reactors. Nuclear Technology, vol. 101, pp. 282-298. March 1993.
- Gido, R.G. Murata, K.K., Smith, R.C., and Washington, K.E., 1996. Burn Modelling Improvements for the CONTAIN Code. Change Document 96, Update C110T. Sandia National Laboratories.
- IDCOR, 1985. Technical Support for Issue Resolution. Technical Report 85.2.

Keinänen, J., 1996. Kiehuvesireaktorilaitoksen suojarakennuksen käyttäytyminen onnettomuustilanteissa. Diplomityö. Teknillinen Korkeakoulu. 1.7.1996.

Kmetyk, L.N., 1993. MELCOR 1.8.2 Assessment: IET Direct Containment Heating Tests. SAND93-2475. Sandia National Laboratories. Oct. 1993.

Lindholm, I., Hedberg, K., Thomsen, K., and Ikonen, K., On Core Debris Behaviour in the Pressure Vessel Lower Head of Nordic Boiling Water Reactors. Technical Report NKS/RAK-2(97)TR-A4, October 1997.

Magallon, D., and Hohman, H., 1993. High Pressure Corium Quenching Tests in FARO. Proceedings of the CSNI Specialist Meeting on Fuel-Coolant Interactions Held in Santa Barbara, California, USA, January 5-8, 1993. NUREG/CP-0127, NEA/CSNI/R(93)8.

Magallon, D., Huhtiniemi, I., and Annunziato, A., 1997. The FARO Programme, Recent Results and Synthesis. Summary of Presentation at the CSARP Meeting Organised by US-NRC at Residence Inn Marriott, Bethesda, Maryland, May 5-8, 1997.

Murata, K.K., Garrol, D.E., Washington, K.E., Gelbard, F., Valdez, G.D., Williams, D.C., and Bergeron, D., 1990. User's Manual for CONTAIN 1.1. A Computer Code for Severe Nuclear Reactor Accident Containment Analyses. Revised for Revision 1.11. NUREG/CR-5026 (SAND87-2309). Sandia National Laboratories. Nov. 1989, Revised July 1990.

NEA, 1996. High Pressure Melt Ejection (HPME) and Direct Containment Heating (DCH). State-of-the-Art Report. Fauske&Associates, Inc. and Sandia National Laboratories in Collaboration with an NEA Group of Experts. NEA/CSNI/R(96)25. December 1996.

Pilch, M.M., Yan, H., and Theofanous, T.G., 1994a. The Probability of Containment Failure by Direct Containment Heating in Zion. NUREG/CR-6075 (SAND93-1535), Sandia National Laboratories. July 1994.

Pilch, M.M. Allen, M.D., Knudson, D.L., Stamps, D.W., and Tadios, E.L., 1994b. The Probability of Containment Failure by Direct Containment Heating in Zion, Supp. 1. NUREG/CR-6075 (SAND93-1535), Sandia National Laboratories. July 1994.

Powers, D. A., Brockmann, J.E., and Shiver, A.W., 1986. VANESA: A Mechanistic Model of Radionuclides Release and Aerosol Generation During Core Debris Interaction with Concrete. NUREG/CR-4308 (SAND85-1370), Sandia National Laboratories, Albuquerque, NM, July 1986.

Summers, R. M., et al., 1994. MELCOR Computer Code Manuals. NUREG/CR-6119(SAND-2185), Sandia National Laboratories. 1994.

Sjövall, H., 1997. Treatment of High Pressure Melt Ejection in Olkiluoto 1 and 2. Level 2 PSA. Teollisuuden Voima Oy (TVO). Letter from Heikki Sjövall, 15 October, 1997.

Tarbell, W.W., Pilch, M., Ross, J.W., Oliver, M.S., Gilbert, D.W., and Nichols, R.T., 1991. Pressurized Melt Ejection into Water Pools. NUREG/CR-3916, SAND84-1531, Sandia National Laboratories, Albuquerque, NM, March 1991.

Washington, E., 1993. Description of the CONTAIN Direct Containment Heating Model. C110U Code Change Document. Sandia National Laboratories. January 1993.

Washington, K. E., and Williams, D. C., 1995. Direct Containment Heating Models in the CONTAIN Code. SAND94-1073, UC-610, Sandia National Laboratories. August 1995.

Williams, D. C., Bergeron, K.D., Carroll, D.E., Gasser, R.D., Tills, J.L., and Washington, K.E., 1987. Containment Loads Due to Direct Containment Heating and Associated Hydrogen Behaviour: Analysis and Calculations with the CONTAIN Code. NUREG/CR-4896 (SAND87-0633). Sandia National Laboratories. May 1987.

Williams, D. C., and Griffith, R. O., 1996. Assessment of Cavity Dispersal Correlations for Possible Implementation in the CONTAIN Code. SAND94-0015, UC-610, Sandia National Laboratories. February 1996.

## **DISTRIBUTION:**

Beredskabsstyrelsen

Attn: Björn Thorlaksen  
Louise Dahlerup

P.O.Box 189  
DK-3460 Birkerød

Risø National Laboratory

Attn: Povl Ölgaard  
Frank Höjerup  
Knud Ladekarl Thomsen

P.O.Box 49  
DK-4000 Roskilde

Finnish Center of Radiation  
and Nuclear Safety

Attn: Lasse Reiman (3)  
Kalevi Haule  
Timo Karjunen  
Juhani Hyvärinen

P.O.Box 14  
FIN-00881 Helsinki

Teollisuuden Voima Oy

Attn: Markku Friberg  
Heikki Sjövall  
Seppo Koski  
Risto Himanen

FIN-27160 Olkiluoto

IVO International Ltd

Attn: Harri Tuomisto  
Petra Lundström  
Olli Kymäläinen

FIN-01019 IVO

Jussi Vaurio

Loviisan Voimalaitos

P.O.Box 23  
FIN-07901 Loviisa

Björn Wahlström

VTT Automation

P.O.Box 13002  
FIN-02044 VTT

VTT Energy

Attn: Lasse Mattila  
Ilona Lindholm (8)  
Risto Sairanen (5)  
Kari Ikonen  
Esko Pekkarinen  
Ari Silde (8)

P.O.Box 1604  
FIN-02044 VTT

Tord Walderhaug  
Geislavarnir Ríkisins  
Laugavegur 118 D  
IS-150 Reykjavik

Institut för Energiteknik

Attn: Egil Stokke  
Oivind Berg

P.O.Box 175  
N-1750 Halden

Sverre Hornkjøl  
Statens Strålevern  
P.O.Box 55  
N-1345 Österås

Swedish Nuclear Power Inspectorate

Attn: Wiktor Frid (5)  
Oddbjörn Sandervåg  
Gert Hedner  
Ninos Garis

S-10658 Stockholm

Vattenfall Energisystem AB

Attn: Klas Hedberg  
Veine Gustavsson

P.O.Box 528  
S-16216 Stockholm

Forsmarks Kraftgrupp AB

Attn: Gustaf Löwenhielm (2)  
Henning Danielsson

S-74203 Östhammar

Kenneth Persson (3)

Vattenfall AB  
Ringhalsverket  
S-43022 Väröbacka

Emil Bachofner (3)  
OKG AB  
S-57093 Figeholm

Jan-Anders Svensson (3)  
Barsebäck Kraft AB  
P.O.Box 524  
S-24625 Löddeköpinge

Studsvik Eco & Safety AB  
Attn: Lars Nilsson (4)  
Lise-Lotte Johansson  
S-61128 Nyköping

ABB Atom AB  
Attn: Yngve Waaranperä  
Timo Okkonen  
S-72163 Västerås

ES-Konsult AB  
Attn: Erik Söderman  
Ferenc Muller  
P.O.Box 3096  
S-16103 Bromma

Lennart Hammar  
ES-Konsult AB  
c/o Dalvägen 63A  
S-18733 Täby

Antti Vuorinen  
Otakallio 2 B 22  
FIN- 02150 Espoo

Kjell Andersson  
Karinta Konsult HB  
P.O.Box 6048  
S-18306 Täby

Torkel Bennerstedt  
NKS  
PL 2336  
S-76010 Bergshamra

Royal Institute of Technology  
Attn: Bal Raj Sehgal  
T. N. Dinh  
R. R. Nourgaliev

Nuclear Power Safety  
S-10044 Stockholm

U.S. Nuclear Regulatory Commission  
Attn: Charles Ader  
Sudhamay Basu  
Washington, DC 20555  
U.S.A

Brian Turland  
233/A32  
AEA Technology  
Winfrith  
Dorchester  
Dorset DT2 8DH  
UK

Sandia National Laboratories  
Attn. Randy Gauntt  
Kenneth E. Washington  
Martin M. Pilch  
Albuquerque  
NM 87185-5800  
U.S.A

Casimir A. Kukielka  
PP&L  
2Nth 9<sup>th</sup> St.  
Allentown  
PA 18101  
U.S.A

Oak Ridge National Laboratory  
Attn. Stephan Hodge  
Robert Sanders  
P.O.Box 2009  
Oak Ridge  
Tennessee 37831-8057  
U.S.A

Martin Sonnenkalb  
Gesellschaft für Anlagen und  
Reactorsicherheit (GRS)  
Schwertnergeste 1  
50667 Köln  
Germany

P.J.T Bakker  
KEMA Nederland B.V.  
Utrechtseweg 310  
6800 ET Arnhem  
Nederland

Karsten Fischer  
Battelle Ingenieurtechnik GmbH  
Düsseldorfer Strasse 9  
65760 Eschborn  
Germany

W. Scholtysek  
Forschungszentrum Karlsruhe GmbH  
Postfach 3640  
D-76021 Karlsruhe  
Germany